lecture 5.1.2012

cluster physics, we had so far:

- methods of cluster production

today:

- details with respect to detection
- binding in clusters and their appearances in mass spectra
    - a) undirected van-der-Waals bonding

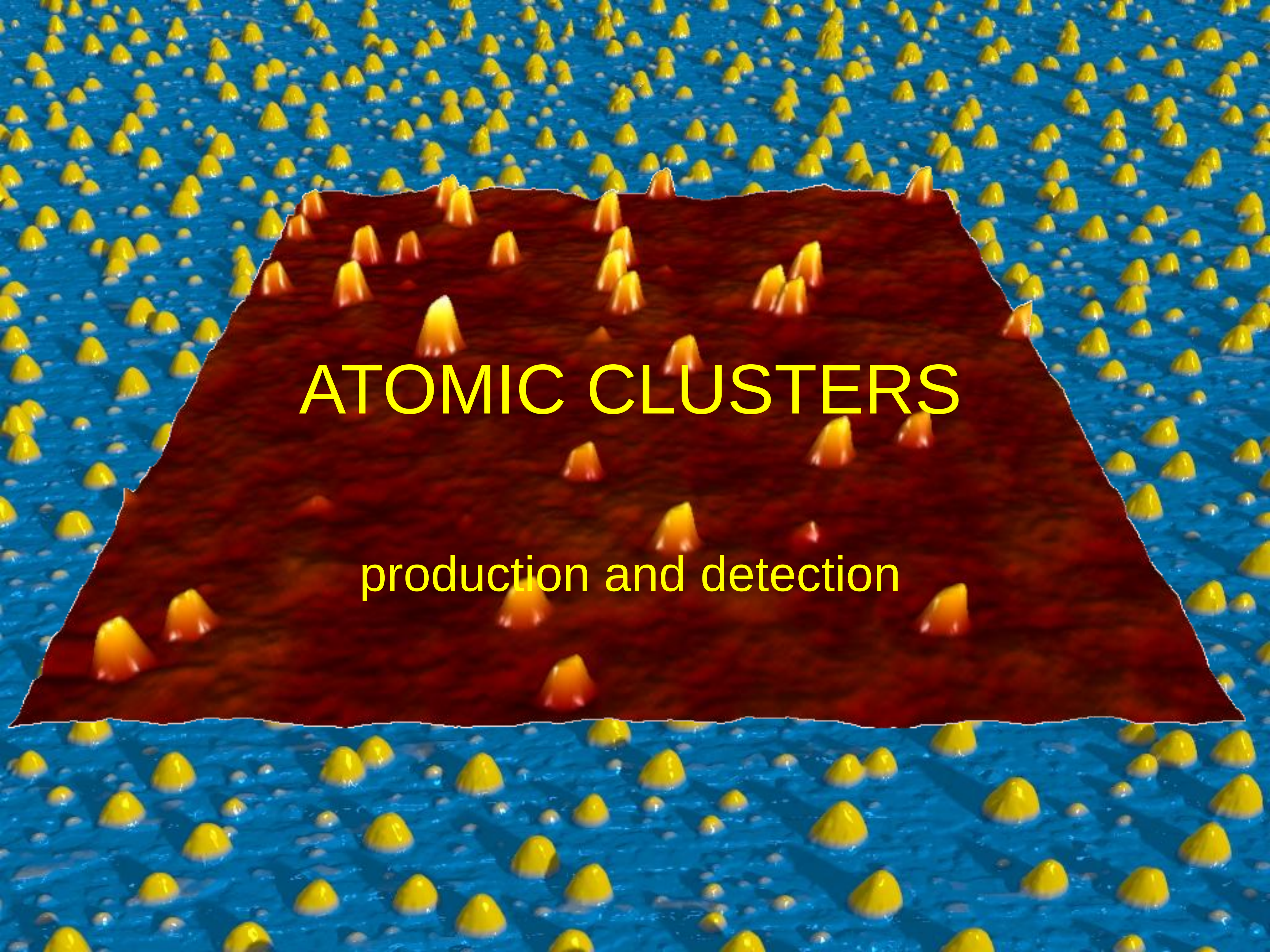

ATOMIC CLUSTERS

production and detection

nanofabrication

- big→ small: „top down“
- atoms → nanostructures: „ bottom up“

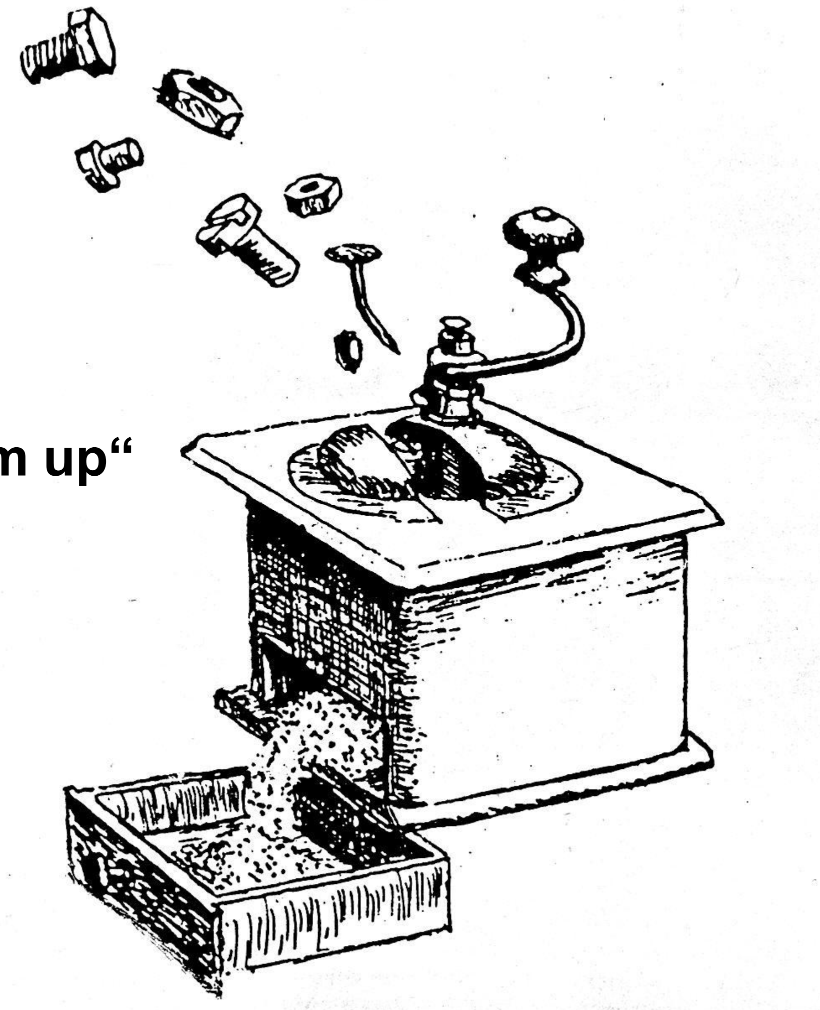

compilation of cluster sources, see last lecture:

a) aggregation of a gas by supersonic expansion

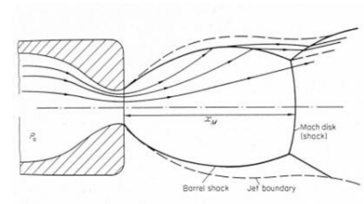

b) laser vaporization followed by expansion

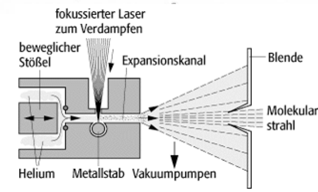

c) plasma generation by arc discharge

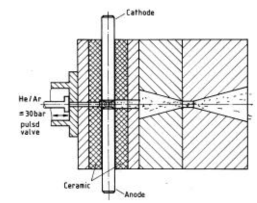

d) sputtering, or magnetron sputtering

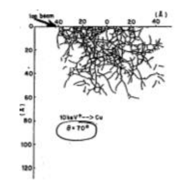

e) electrospray ion source

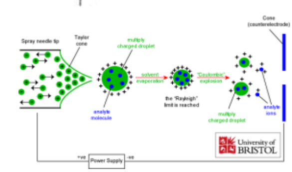

f) Helium droplet pick-up source

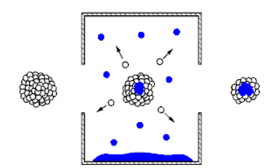

How to see the clusters -
Components of a mass spectrometer

Ionisation

Ion Source

Electron Ionisation (EI)

Chemical Ionisation (CI)

Fast Atom Bombardment (FAB)

Electrospray Ionisation (ESI)

Laser Vaporization

Matrix-Assisted Laserdesorption

Ion Separation

Mass Analyser

Quadrupole

Magnetic Sector Field

Electric Sector Field

Time-Of-Flight (TOF)

Ion Trap

Ion Detection

Detector

Electron Multiplier

Multichannel plate

Faraday Cup

new: imaging

why m/q and not m ?

- electrical and magnetic fields:
  $F = q(E + v \times B) = ma$

➔ $a = q/m\ (E + v \times B)$
(ions with the same m/q have identical flight paths)

all mass spectrometers determine m/q of an ion

Time of flight (TOF) mass spectrometry

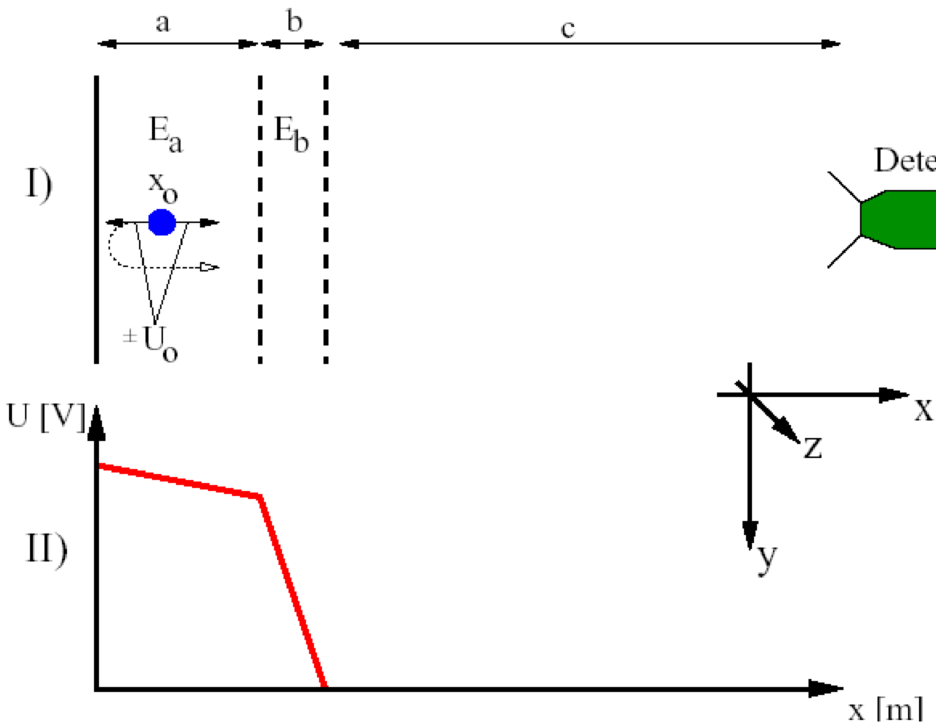

Abbildung 3.7: Feldverlauf und Spannungen im TOF
I) *Aufbau eines 2-stufigen TOF. In den Bereichen a und b werden die Teilchen ausgehend von ihrem Startort x_0 durch die Felder E_a und E_b beschleunigt. Ist ihre Anfangsenergie U_0 entgegen dem Feldgradienten gerichtet, wird das Teilchen umgelenkt (gepunktete Linie). Bei hinreichend großen Werten von U_0 ist dies als Aufspaltung der Massenlinien im Spektrum zu beobachten. Nach einer feldfreien Driftstrecke c treffen die Ionen auf den Detektor und werden dort nachgewiesen. Die Geschwindigkeit aus der Überschall-Expansion wird in die Simulation nicht einbezogen, da sie senkrecht auf dem Vektor der Beschleunigungsrichtung steht und somit keinen Einfluß auf die Flugzeit hat. Lediglich die Transmission (s. Kap. 3.4.3) wird durch sie beeinflußt.* **II)** *Spannungsverlauf im TOF.*

Time-of flight (TOF) mass spectrometry

$$x(t) = x_0 + v_0 \times t + \frac{b_a}{2} \times t^2 \tag{3.3}$$

mit der Anfangs-Geschwindigkeit v_0 und der Beschleunigung b_a, die sich folgendermaßen durch die Anfangsenergie U_0 und die Feldstärke E_a ersetzen lassen:

$$v_0 = \sqrt{\frac{2U_0}{m}}, \quad b_a = \frac{Ze}{m} E_a \tag{3.4}$$

$Ze \equiv q$ ist die auf dem Cluster akkumulierte Ladung. Die Z-fache Aufladung mit $Z > 1$ wird nur bei der Wechselwirkung der Teilchen mit intensiven Laserstrahlen beobachtet. Als Lösung ergeben sich für die drei Bereiche folgende Gleichungen:

$$\begin{aligned}
t_a &= \frac{\sqrt{2m}}{qE_a}\left[\sqrt{U_0 + q(a-x)E_a} \pm \sqrt{U_0}\right] && (3.5)\\
t_b &= \frac{\sqrt{2m}}{qE_b}\left[\sqrt{U_0 + q(a-x)E_a + qbE_b} - \sqrt{U_0 + q(a-x)E_a}\right] && (3.6)\\
t_c &= c\sqrt{\frac{m}{2(U_0 + q(a-x)E_a + qbE_b)}} && (3.7)\\
t_{gesamt} &= t_a + t_b + t_c && (3.8)
\end{aligned}$$

effect of an initial spatial distribution

The *space-focus plane*

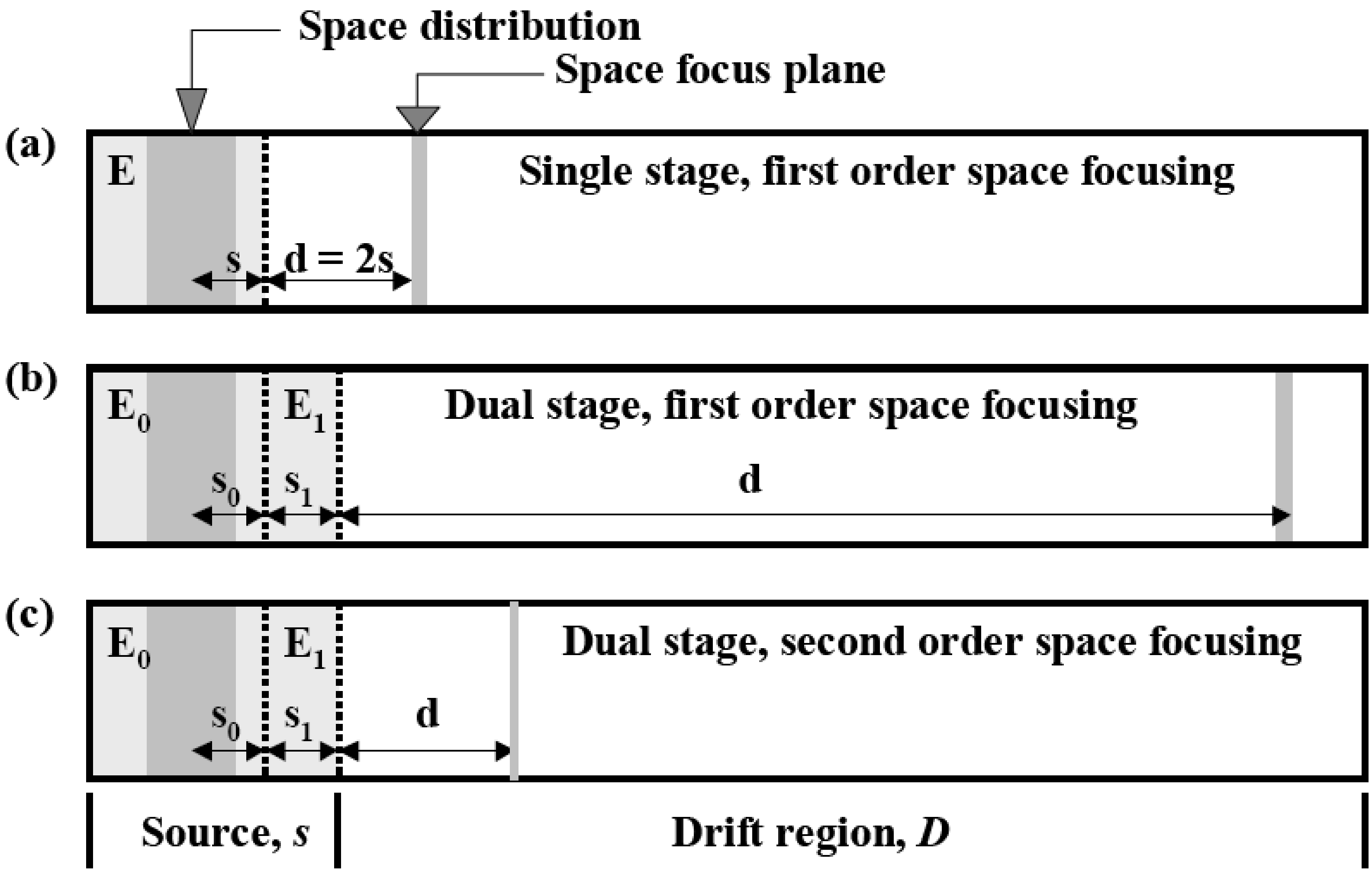

Reflectrons improve mass resolution

Dual-stage reflectron

The original reflectron invented by Boris Mamyrin was a dual stage.

Mamyrin, B. A.; Karataev, V. I.; Shmikk, D. V.; Zagulin, V. A, *Mass reflectron. New nonmagnetic time-of-flight high-resolution mass spectrometer.* **Zhurnal Eksperimental'noi i Teoreticheskoi Fiziki** (1973) **64**, 82-89.

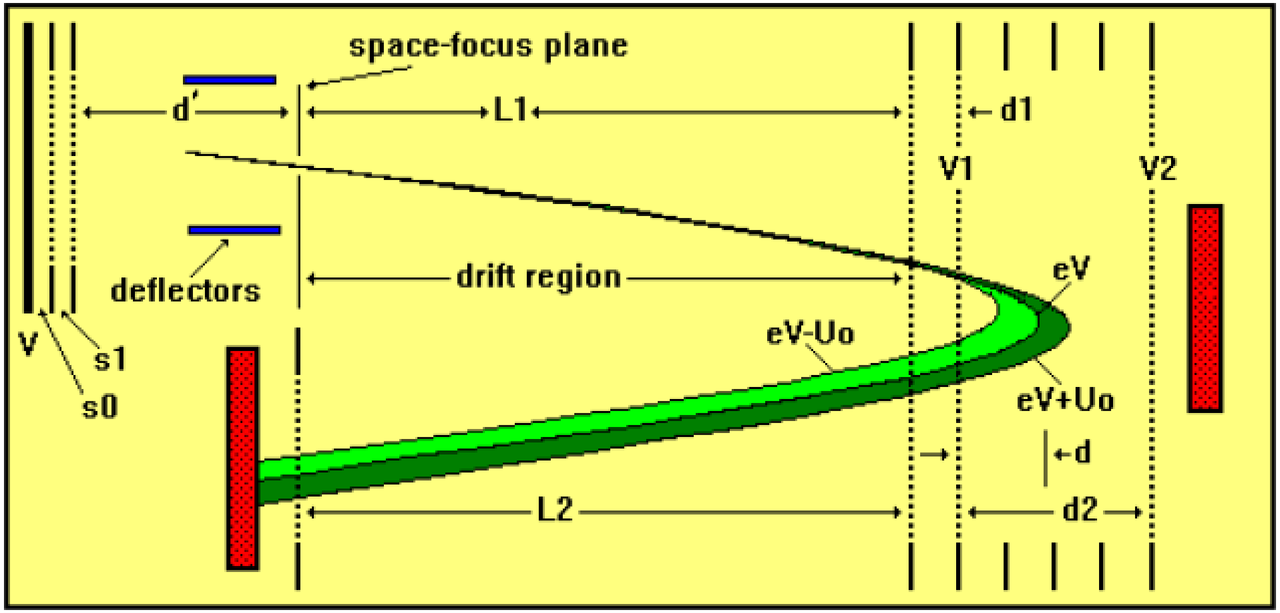

The dual stage reflectron can be designed to achieve second order focusing. In this case the reflectron depth is much smaller than the flight tube length.

Time-of-flight mass spectrometer

here: reflectron-type, own system

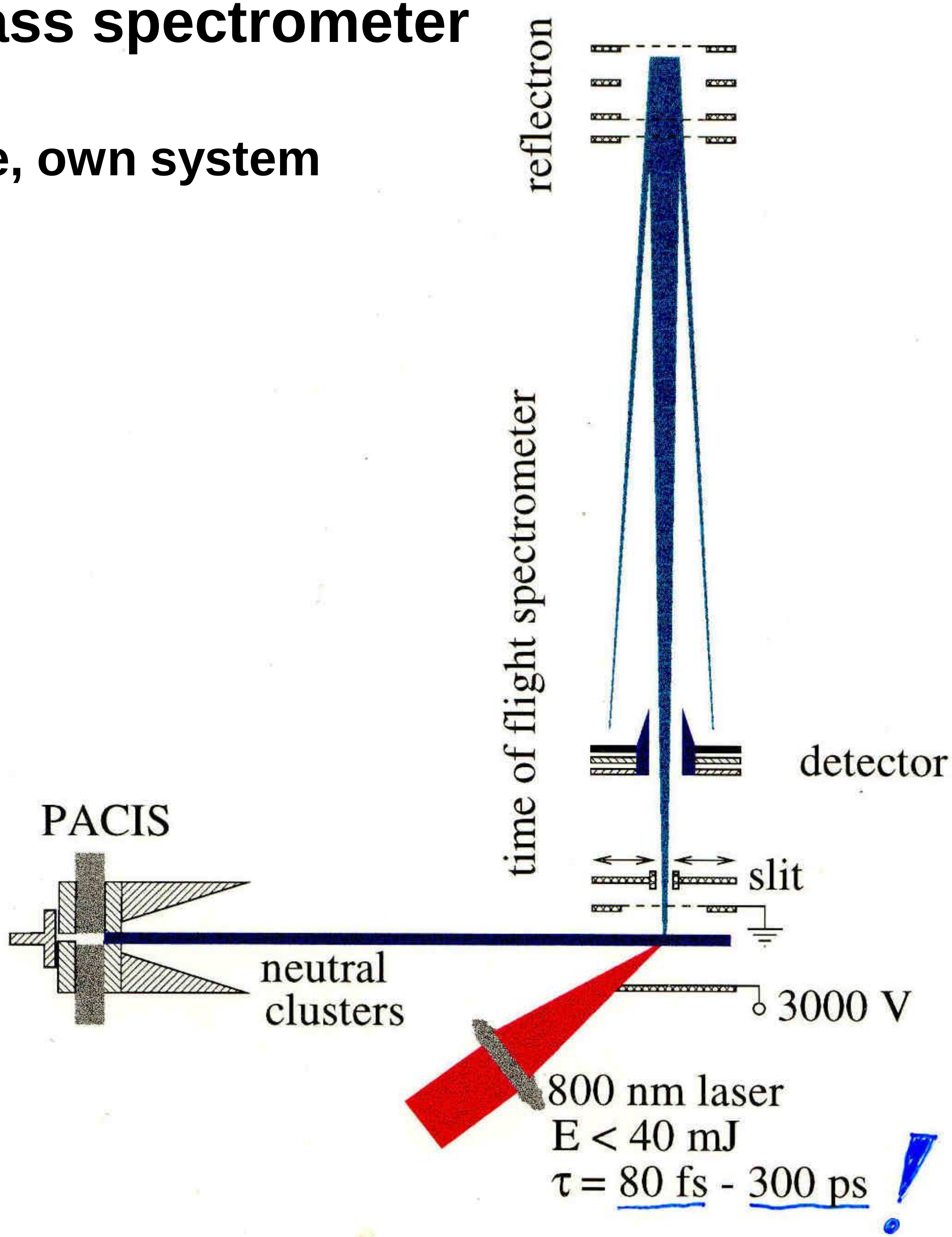

time-of-flight mass spectrum of Pb clusters

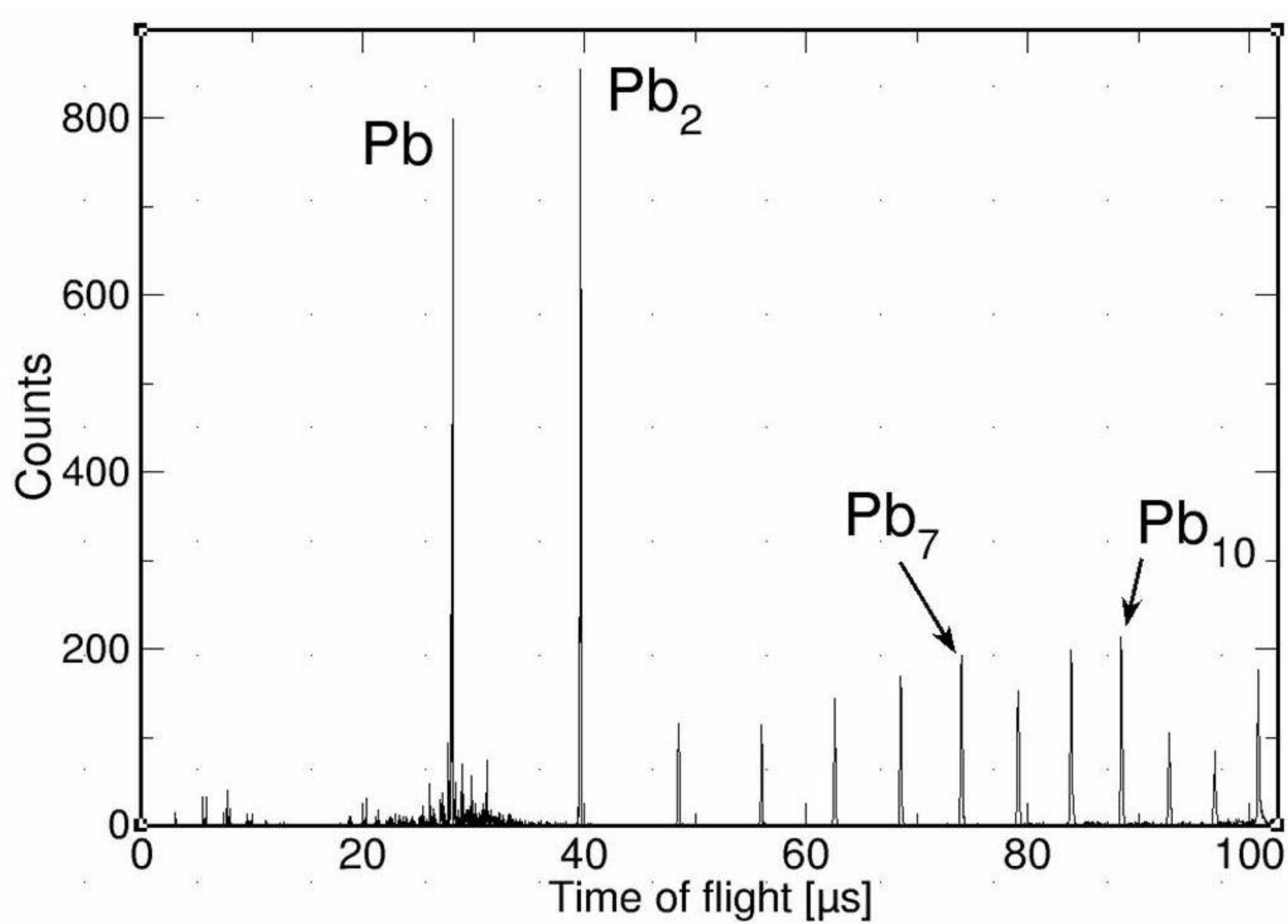

time-of-flight mass spectroscopy

negatively charged Al clusters

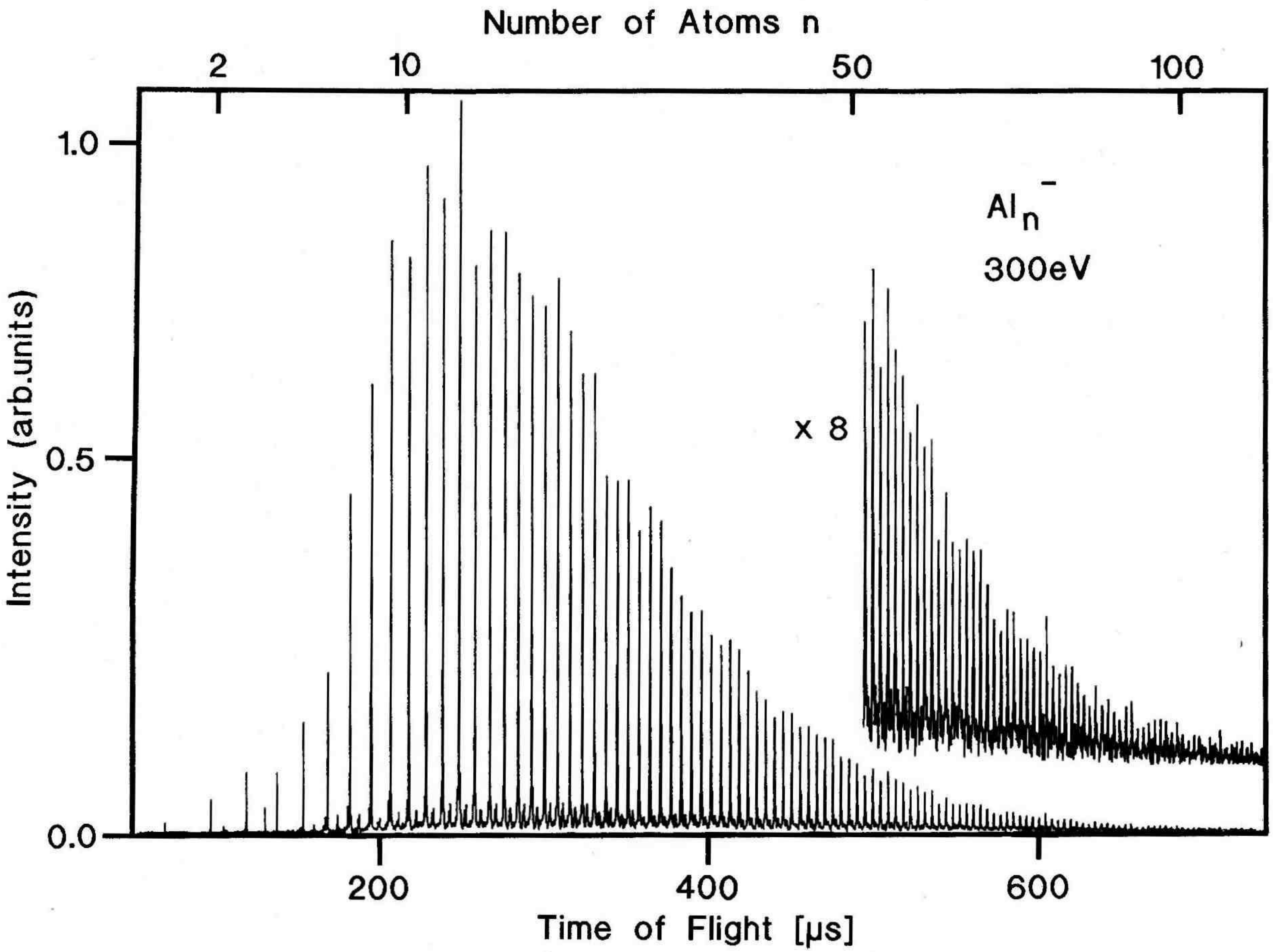

Mg_N grown in large He droplets

note changes in mass scale

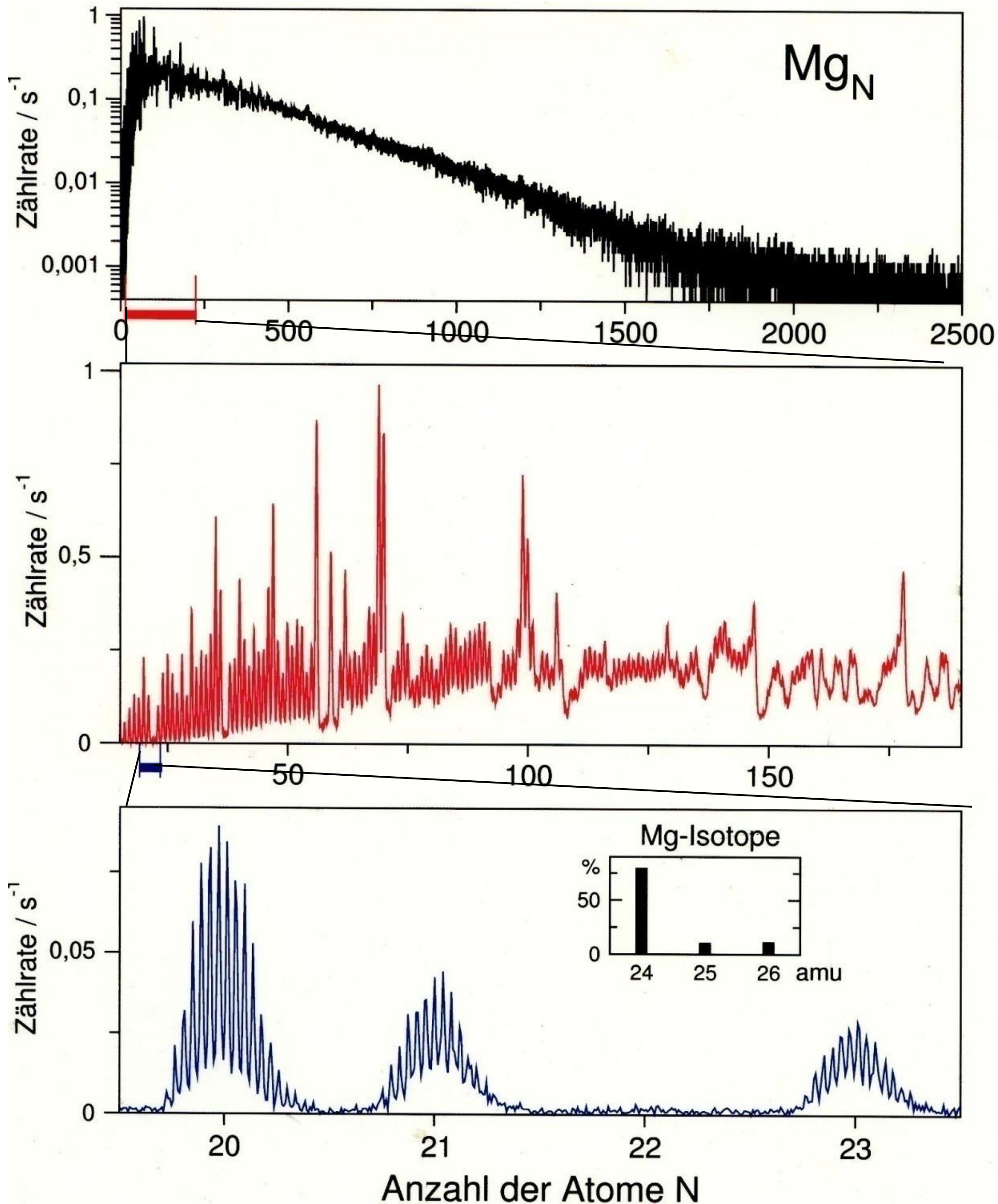

Th. Diederich, T. Döppner, Th. Fennel, J. Tiggesbäumker und K.-H. Meiwes-Broer Phys. Rev. A **72**:023203, 2005

mass spectrum shows quantum effects

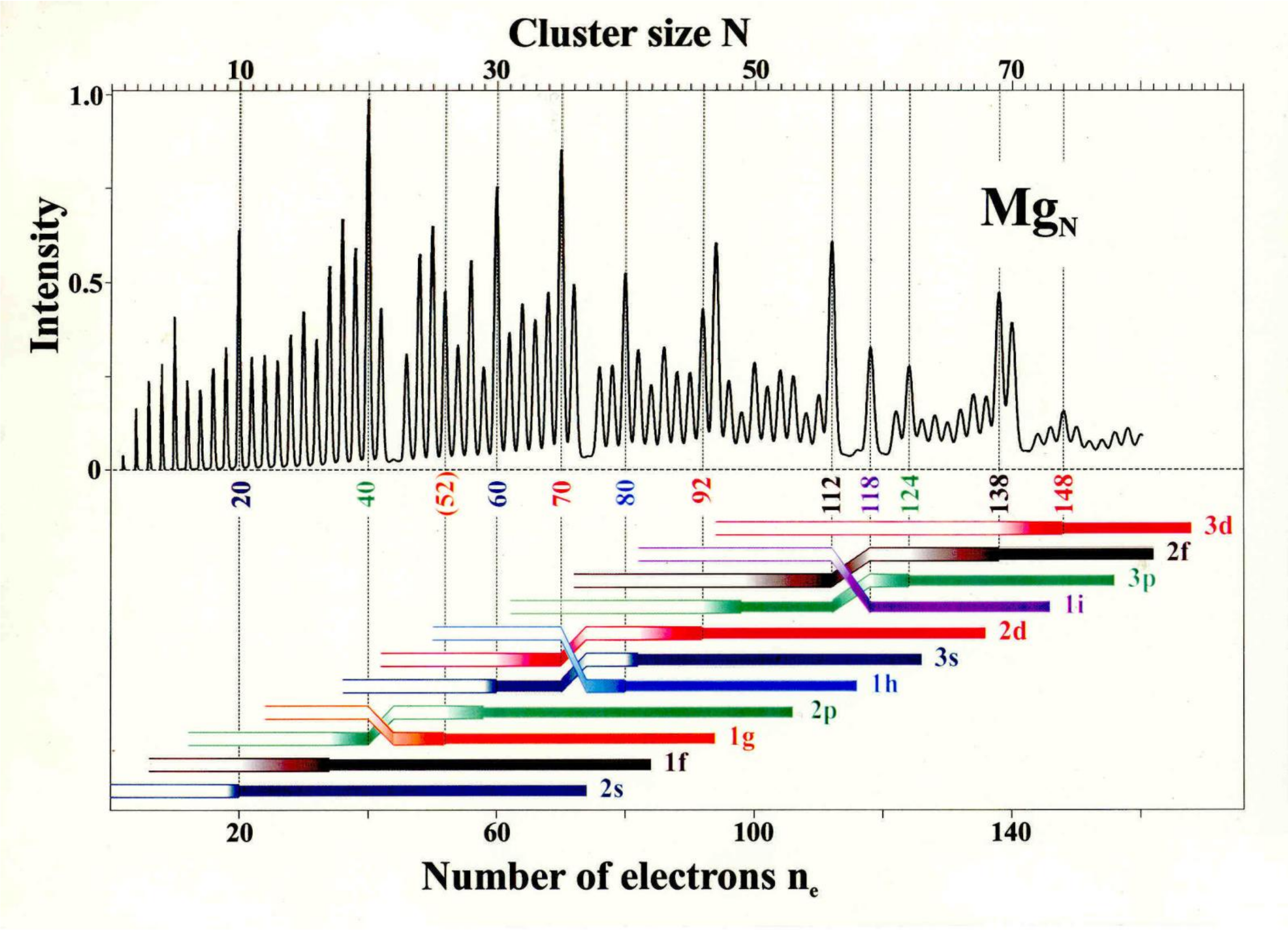

Diederich *et al.* PRL 86, 4807 (2001)

another method to see clusters: microscopy

3 – 10 nm Cobalt particles in the scannig tunneling microscope

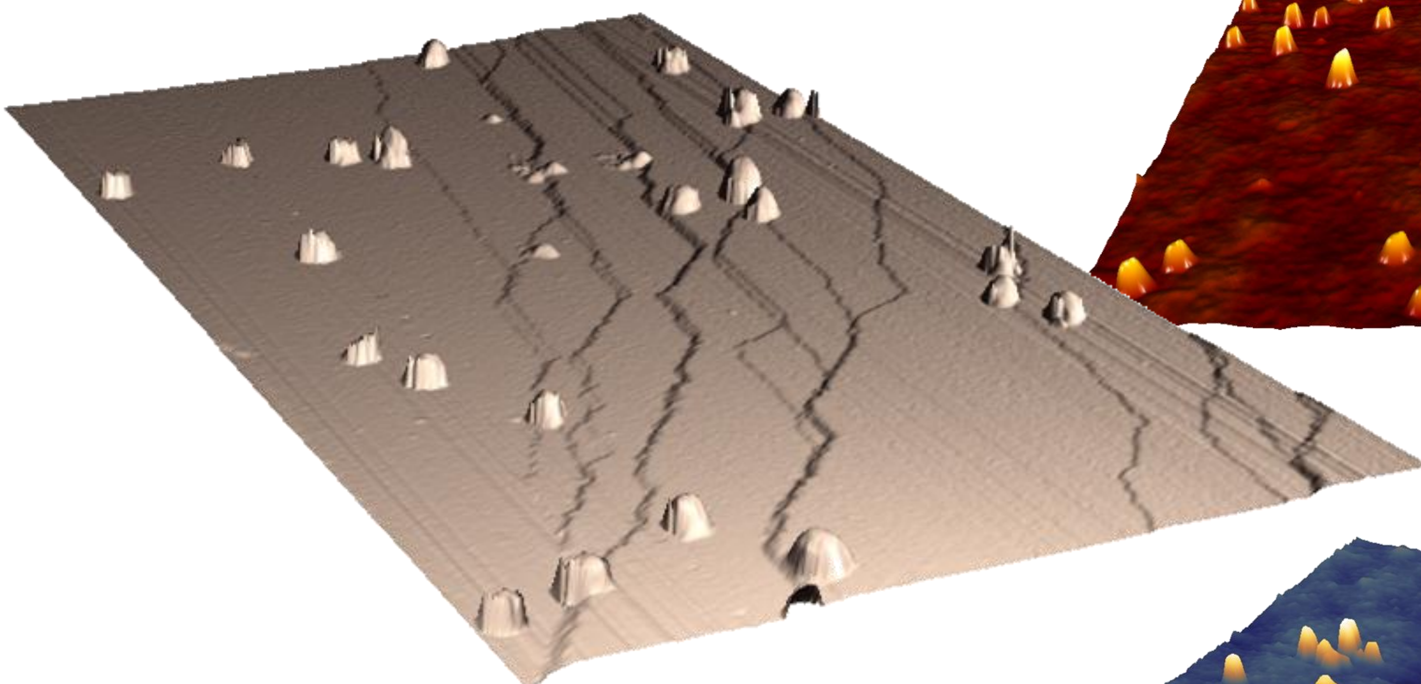

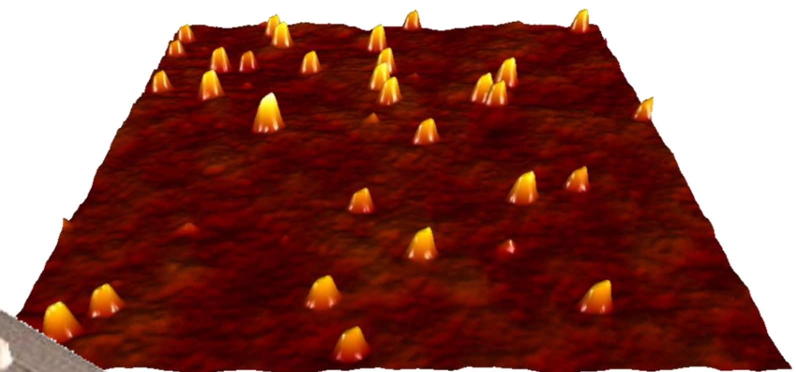

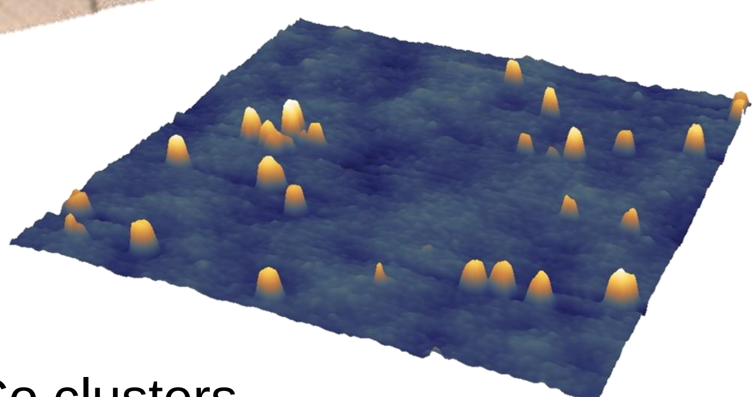

7 nm Co clusters

new method:
imaging of single clusters with XUV or X ray radiation

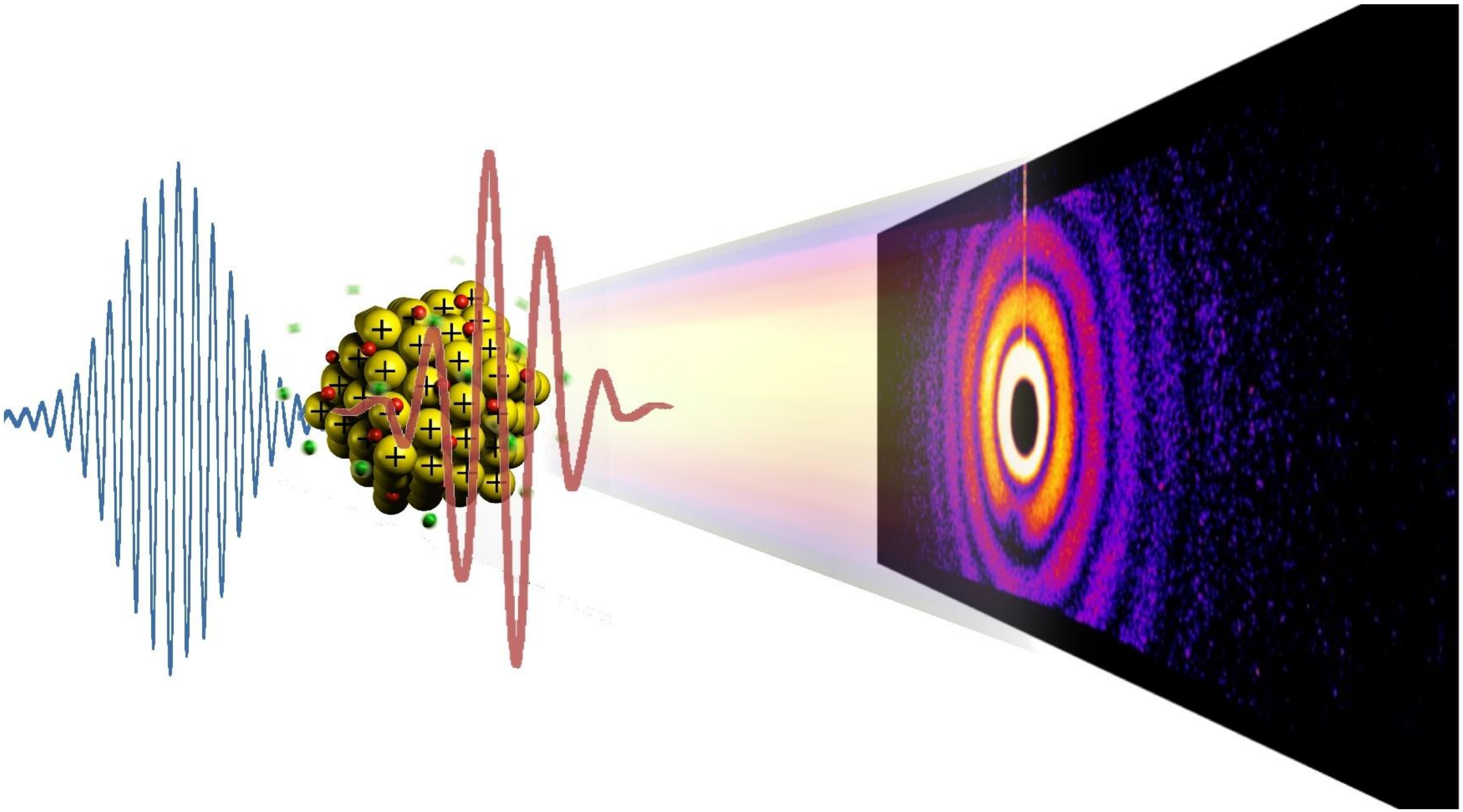

Mie scatering by nm particles, Th. Möller, TU Berlin
project currently funded by the BMBF, performed at FLASH and LCLS

imaging of single clusters with XUV or X ray radiation

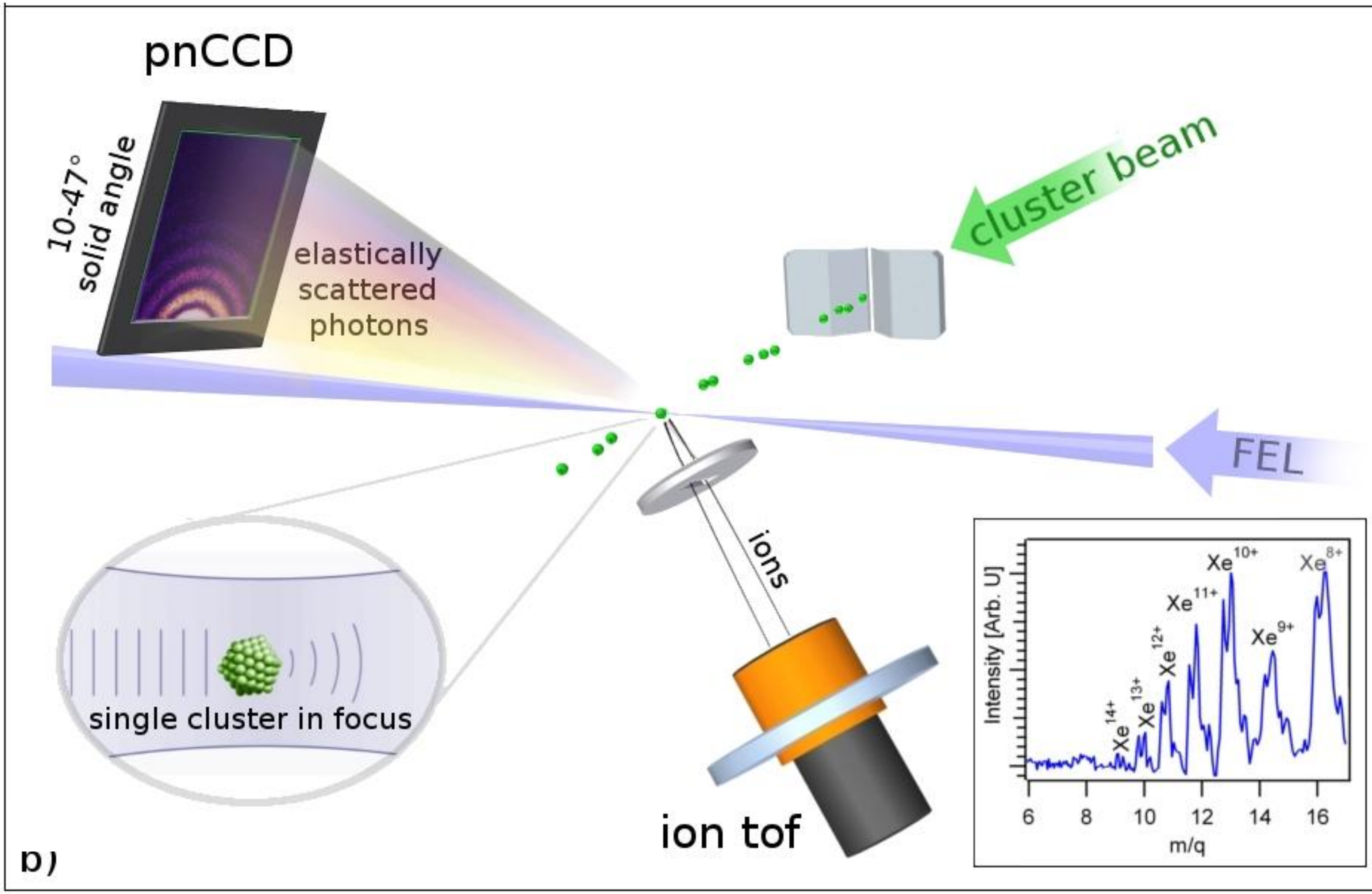

novel technologies:

1. XUV and X-ray pulses with 10^{12} photons per pulse or more, within 10 fs
2. fast detector with thousands of pixels (an MCP does not help, why not?)

imaging of single clusters with XUV or X ray radiation

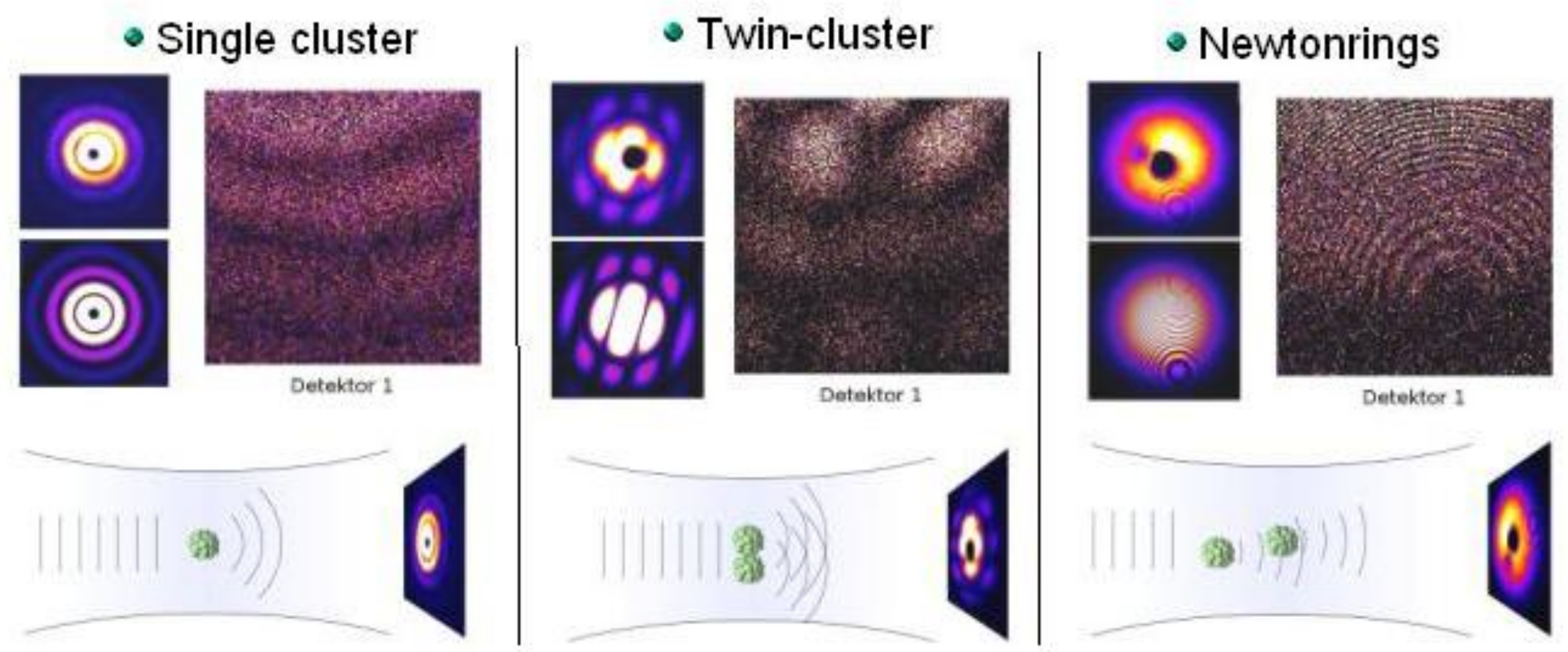

goal: resolving atomic structure with sufficiently high photon energy

binding in clusters and their appearences in mass spectra

a) undirected bonding (Van-der-Waals)

b) ionic

c) covalent

d) metal

Neutral rare-gas clusters

Very weak bonding (van der Waals, or dispersion)

Mostly pair-wise (can be modelled by Lennard-Jones 6-12 potential)

But three-body corrections are non-negligible

Need low temperature to be stable

(dimerization temperature is 11K for He, 281 K for Xe)

Molecular orbital diagram for He dimer

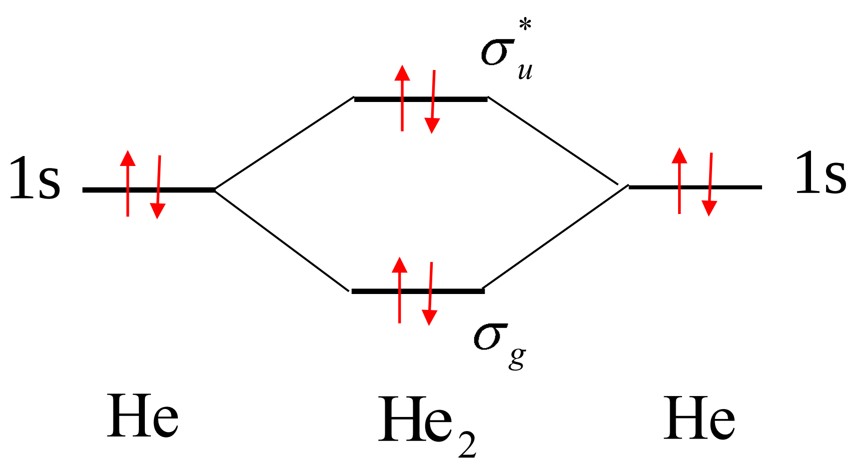

Bond order = 0

charged rare-gas clusters

Molecular orbital diagram for singly charged He dimer

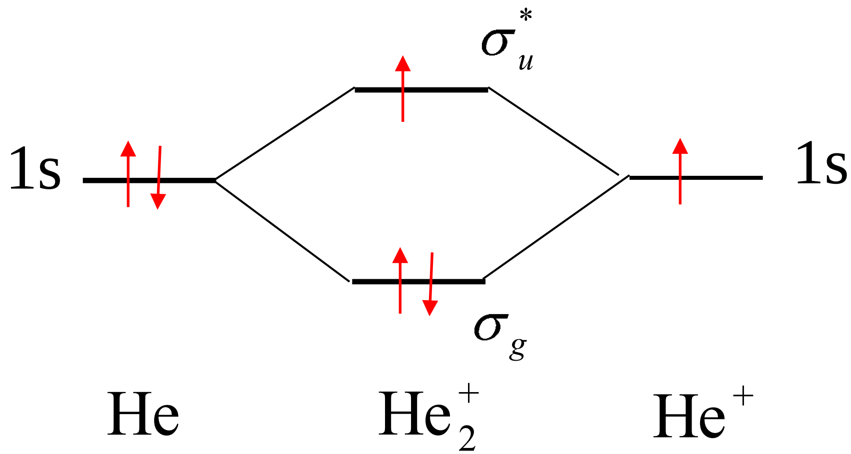

Quite different electronic structure !

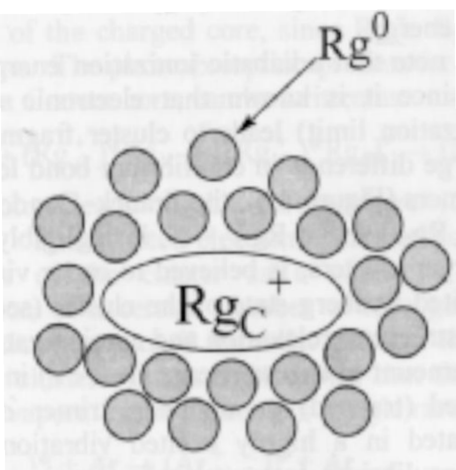

Bond order = 1/2

Reduced bond length

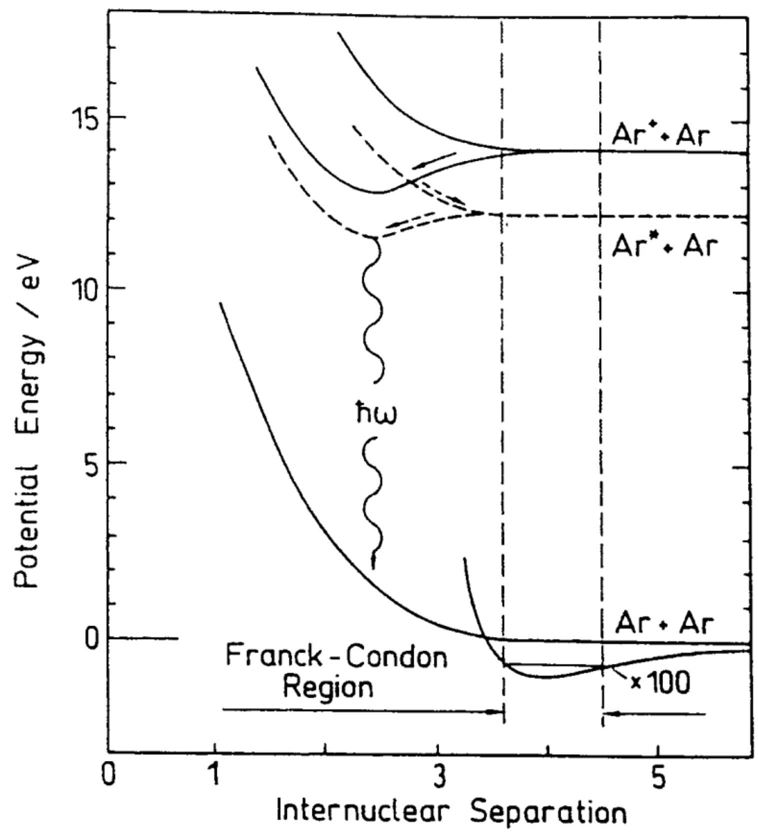

calculation of the structures

- two-body central forces (which is the main restriction)
- N-particle problem, 3N-6 inner coordinates $\boldsymbol{r}^N$
- conjugated momenta $\boldsymbol{p}^N$

Hamilton function

$$H(\boldsymbol{p}^N,\boldsymbol{r}^N) = \Sigma_i\, \boldsymbol{p}_i^2/2m + V(\boldsymbol{r}^N)$$

with $\boldsymbol{r}^N$ vectors in the N-dimensional configuration space

V d W: Lennard Jones Clusters

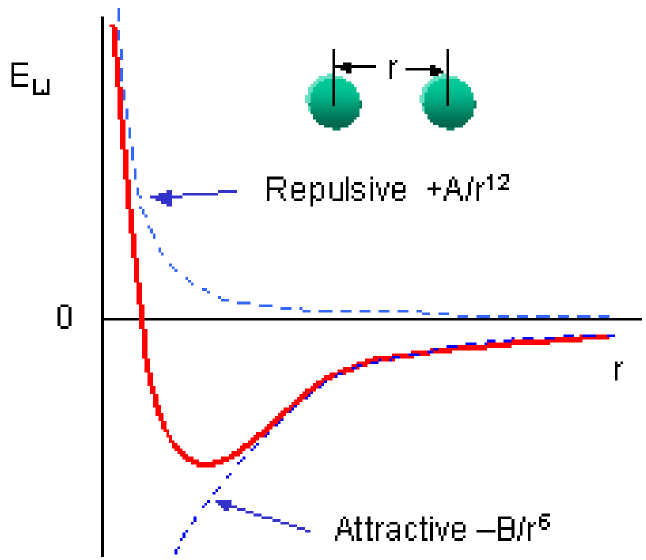

$$u_{LJ}(r) = 4\varepsilon\left[\left(\frac{\sigma}{r}\right)^{12} - \left(\frac{\sigma}{r}\right)^{6}\right]$$

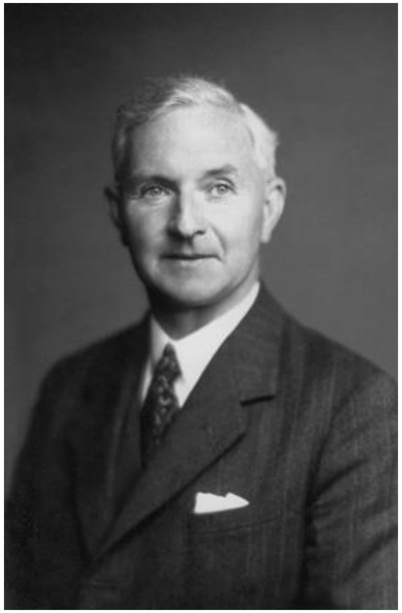

Sir John Lennard Jones

- Spherically-symmetric, pairwise additive model

$$U(\mathbf{r}^N) = \sum_{i=1}^{N}\sum_{j<i} u_{ij}(r_{ij}) \qquad u_{LJ}(r) = 4\varepsilon\left[\left(\frac{\sigma}{r}\right)^{12} - \left(\frac{\sigma}{r}\right)^{6}\right]$$

- Force

$$\mathbf{F}_i = -\sum_{j\neq i}\frac{\mathbf{r}_{ij}}{r_{ij}}\frac{du_{ij}}{dr_{ij}} \qquad \frac{\mathbf{r}}{r}\frac{du_{LJ}}{dr} = \mathbf{r}\,\frac{48\varepsilon}{\sigma^2}\left[\left(\frac{\sigma}{r}\right)^{14} - \frac{1}{2}\left(\frac{\sigma}{r}\right)^{8}\right]$$

Section of a potential energy surface

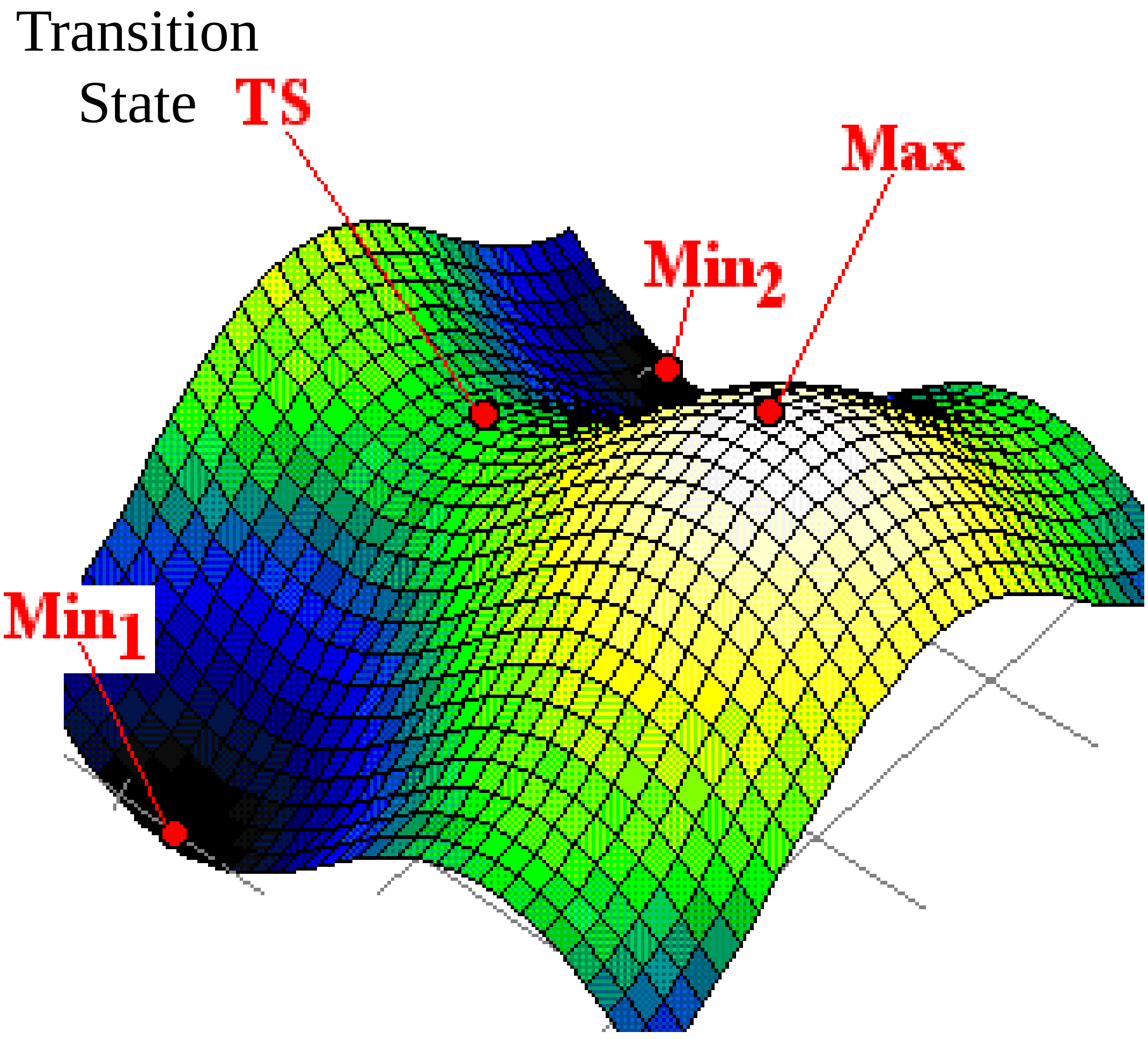

Example: stable and metastable configurations

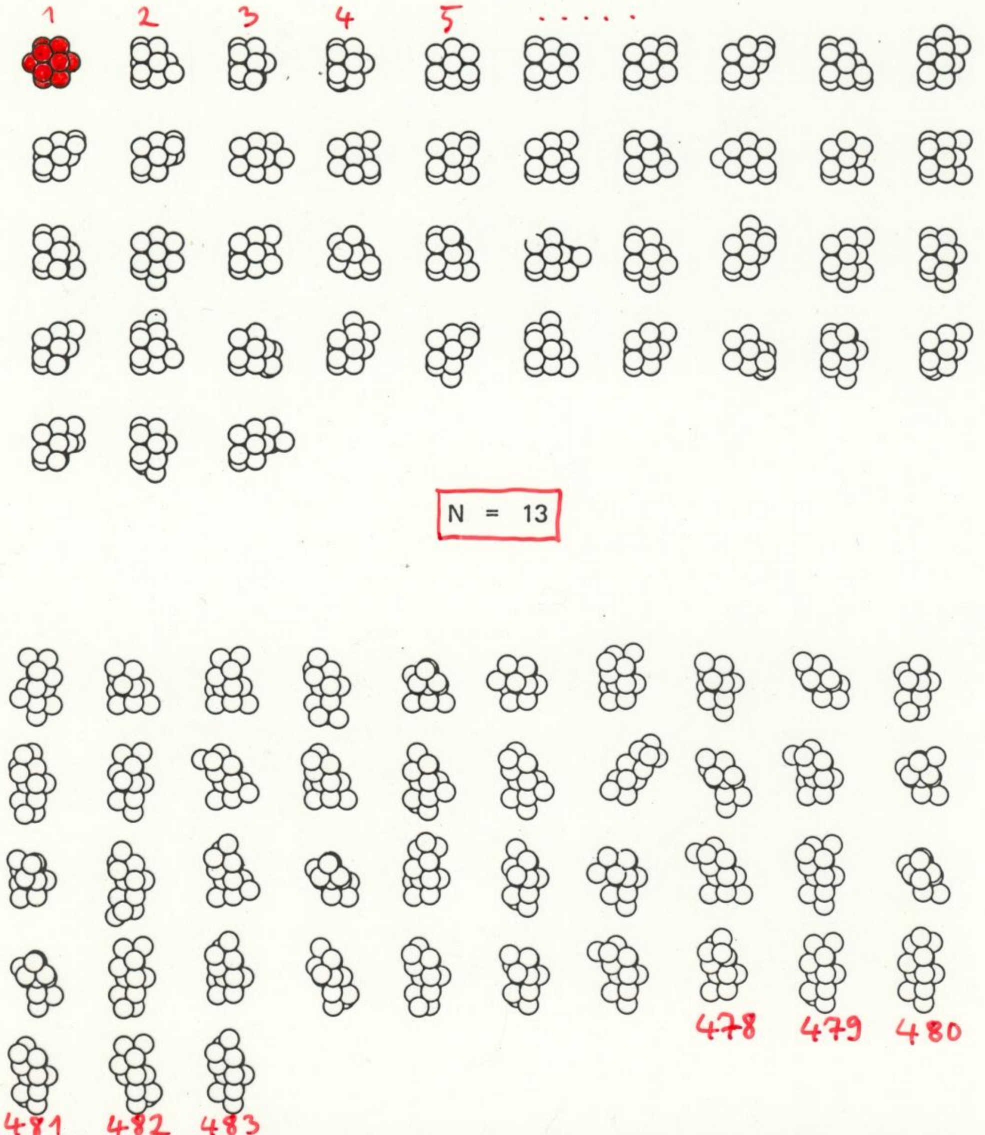

Fig. 11. Tetrahedral Lennard-Jones isomers for $N = 13$. The first and last 43 isomers from the total of 483 are selected, again in order of decreasing binding energy. Note the $N = 13$ icosahedron top left and the Boerdijk spiral, which proves to have by no means the least possible binding energy.

Hoare

local energy minima

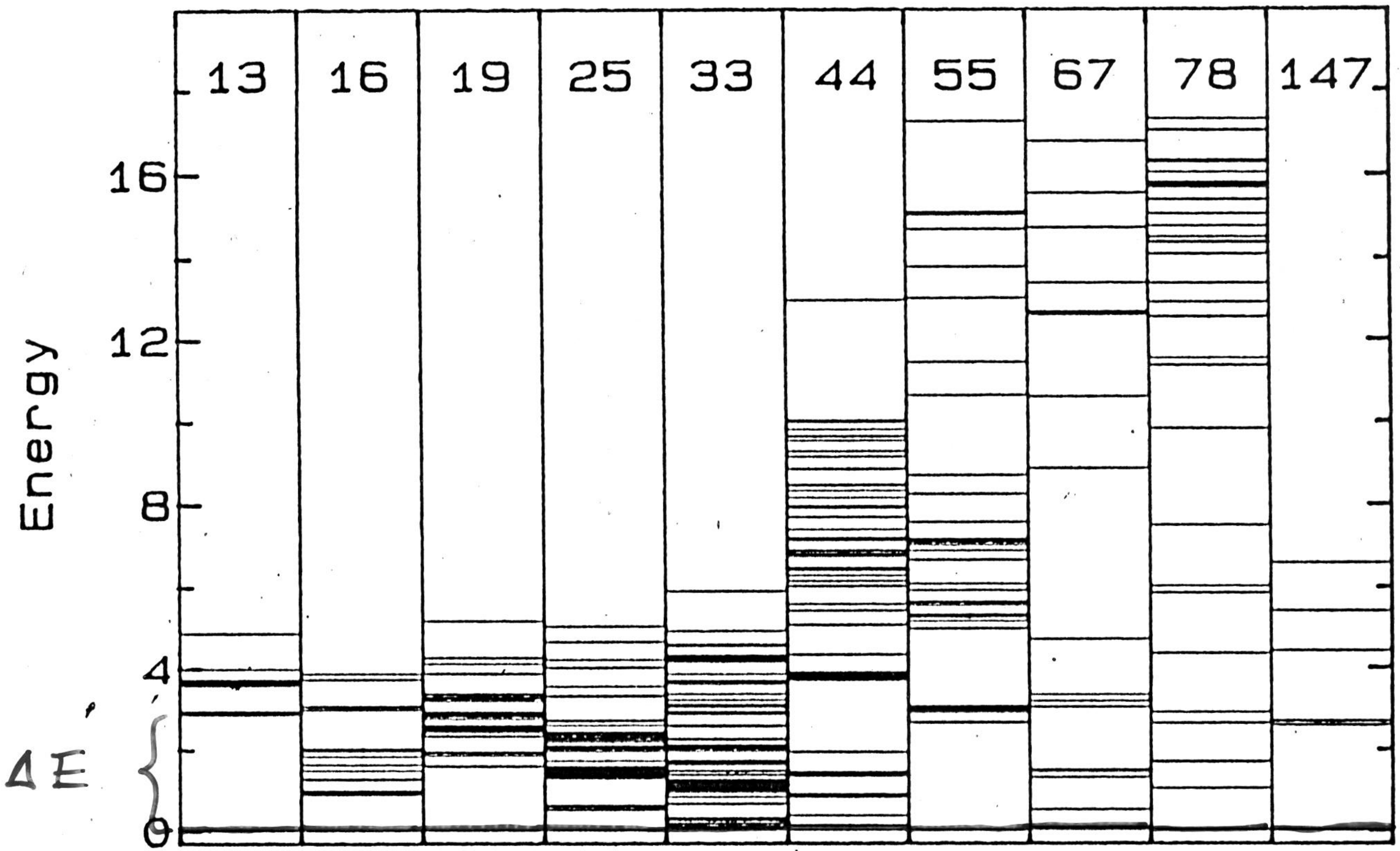

Figure 4. Local energy minima found for clusters containing 13 to 147 atoms. For each cluster size, the zero of energy is taken to be the energy of the apparent ground state. For clusters containing 55 or more atoms, we found minima of higher energy that are not shown.

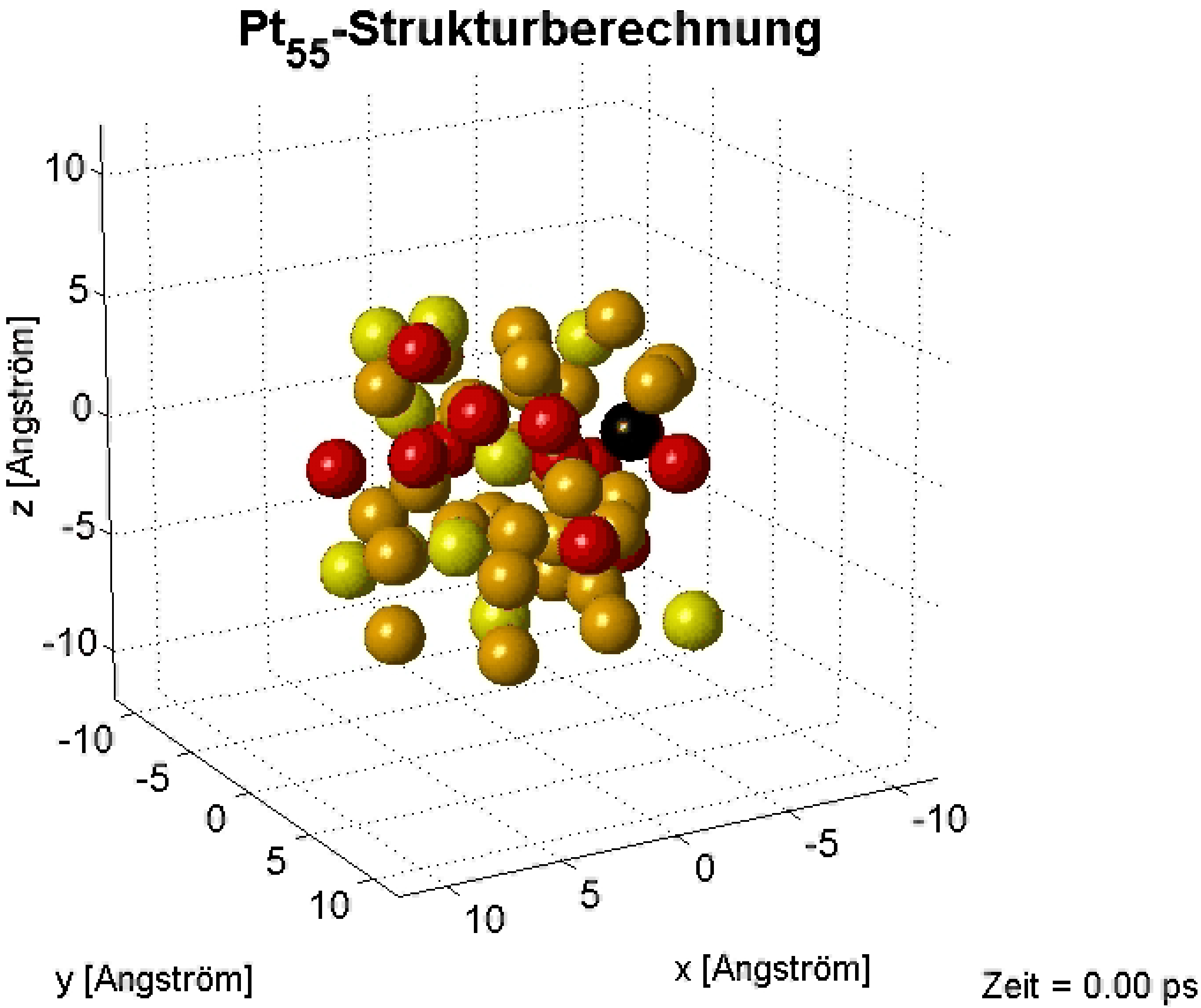

Thomas Fennel

Mackay icosahedra

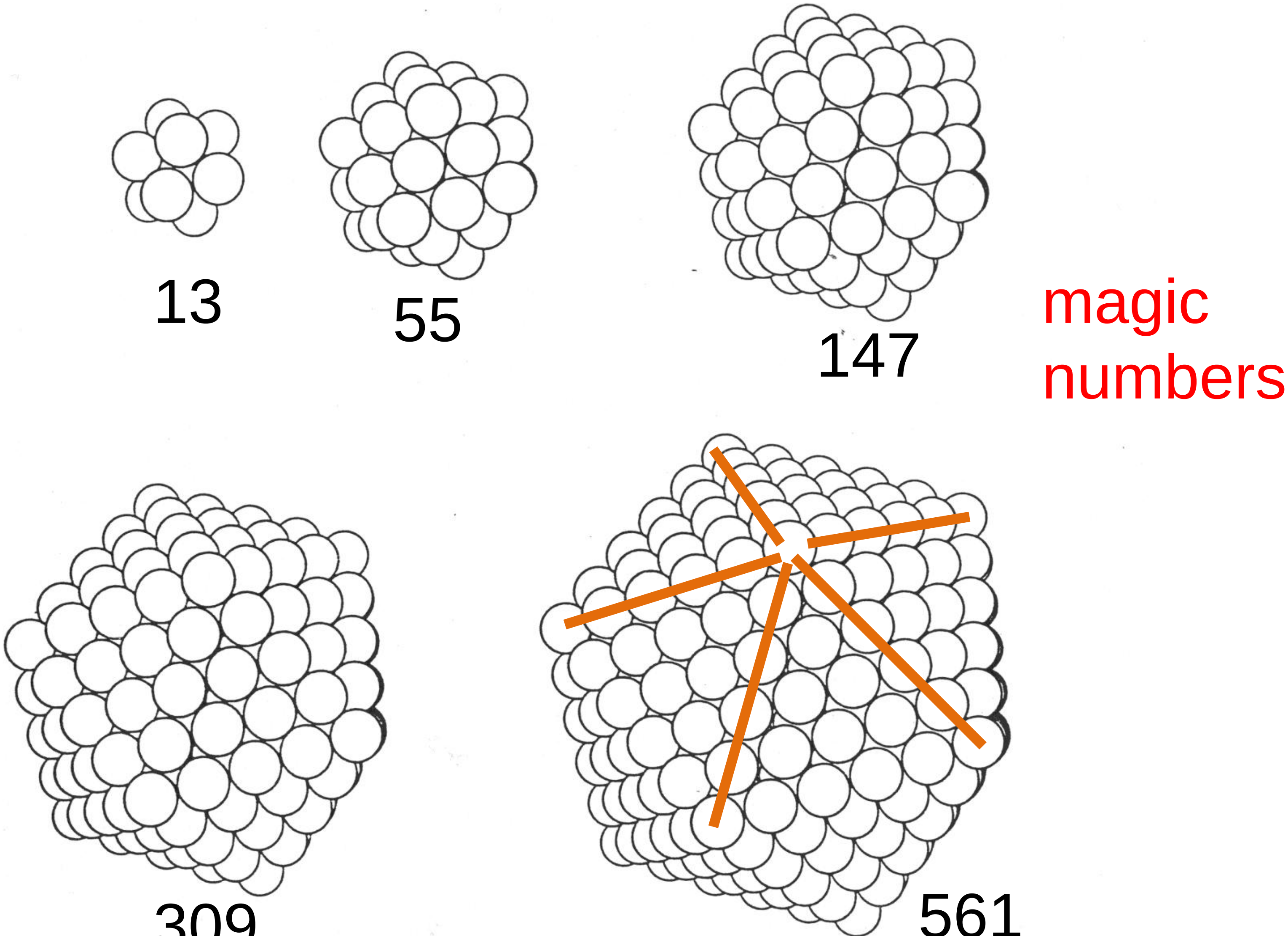

Fig. 5. The first five Mackay icosahedra. $N = 13$, 55, 147, 309, and 561, respectively.

geometric shell structure of rare gas clusters